# Symmetry energy softening in nuclear matter with non-nucleonic constituents

Wei-Zhou Jiang, Rong-Yao Yang, and Dong-Rui Zhang

Phys. Rev. C **87**, 064314 — Published 21 June 2013

DOI: 10.1103/PhysRevC.87.064314

# Symmetry energy softening in nuclear matter with non-nucleonic constituents

Wei-Zhou Jiang*, Rong-Yao Yang, and Dong-Rui Zhang
*Department of Physics, Southeast University, Nanjing 211189, China*

We study the trend of the nuclear symmetry energy in relativistic mean-field models with appearance of the hyperon and quark degrees of freedom at high densities. On the pure hadron level, we focus on the role of $\Lambda$ hyperons in influencing the symmetry energy both at given fractions and at charge and chemical equilibriums. The softening of the nuclear symmetry energy is observed with the inclusion of the $\Lambda$ hyperons that suppresses the nucleon fraction. In the phase with the admixture of quarks and hadrons, the equation of state is established on the Gibbs conditions. With the increase of the quark phase fraction in denser and denser matter, the apparent nuclear symmetry energy decreases till to disappear. This softening would have associations with the observations which need detailed discriminations in dense matter with the admixture of new degrees of freedom created by heavy-ion collisions.

PACS numbers: 21.65.Ef, 21.60.Jz, 21.65.Qr, 13.75.Ev

## I. INTRODUCTION

The nuclear symmetry energy of isospin asymmetric nuclear matter is not only important for understanding the structure of neutron- or proton-rich nuclei and the reaction dynamics of heavy-ion collisions, see, e.g., Ref. [1–3], but also plays a crucial role in a number of important issues in astrophysics, see, e.g., Refs. [4–6]. Recently, appreciable progresses have been achieved on constraining the symmetry energy at saturation and subsaturation densities either through the extraction based on astrophysical observations or in terms of terrestrial data [7–12]. However, the density dependence of the symmetry energy is still poorly known at supranormal densities [3, 13–15]. Theoretical models predict diverse density dependencies of the symmetry energy at high densities. Noticeably, similarly diverse density profile of the symmetry energy can be extracted from analyzing the FOPI/GSI data on the $\pi^-/\pi^+$ ratio in relativistic heavy-ion collisions with various transport models [13–15]. In spite of this inconsistency, the theoretical uncertainty of high-density symmetry energy is regarded to be associated with the tensor force that originates from the exchange terms [16, 17]. In the ladder approximation, the exchange terms can be well treated in the Brueckner theory either in the relativistic or non-relativistic frameworks [18, 19]. In deed, the vacuum polarizations given by ring diagrams are absent in the Brueckner theory. The inclusion of the ring diagrams is however very complicated. In this work, we do not carry on the tensor force that appears beyond the Hartree approximation but consider the non-nucleonic degrees of freedom in the Hartree approximation.

The new degrees of freedom considered here are hyperons and quarks that may appear in dense matter roughly around the density 2-4$\rho_0$, depending on the parametrization of models [20–24]. Nuclear matter at this density domain can be produced via heavy-ion collisions, and it usually includes the admixture of non-nucleonic degrees of freedom. In the past, the symmetry energy effects on these phase transitions have been found to be very significant [23, 25, 26]. However, the effects of new constituents on the symmetry energy are seldom investigated. It is not the aim of this work to resolve the uncertainty of the high-density symmetry energy but to reveal the variation of the symmetry energy in phases mixed with these new constituents. Once the phase transition occurs, the system goes to the mixed phase that can be theoretically constructed by virtue of the phase equilibrium conditions, namely, the Gibbs conditions in this work. In the mixed phase, we define the symmetry energy according to the general expression of the energy density that is different from that in pure nuclear matter. The paper is organized in the following. In Sec.II, we present necessary formulas for the nuclear symmetry energy in pure hadron and mixed phases with the relativistic mean-field (RMF) framework. The construction of the mixed phase of quarks and baryons are presented briefly. In Sec. III, the numerical results and discussion are given. At last, we give a brief summary.

## II. FORMALISM

In the parabolic approximation, the energy per nucleon in isospin asymmetric nuclear matter can be written as

$$\mathcal{E}/\rho_N = E/A = e_0(\rho_N) + E_{sym}(\rho_N)\delta^2, \quad (1)$$

*wzjiang@seu.edu.cn

where $e_0(\rho_N)$ is the energy per nucleon in symmetric nuclear matter with $\rho_N = \rho_n + \rho_p$ being the nucleonic number density, the $E_{sym}(\rho_N)$ is the symmetry energy, and $\delta = (\rho_n - \rho_p)/\rho_N$ is the isospin asymmetry. In RMF models, the energy density can generally be written as

$$\begin{aligned}\mathcal{E} &= \frac{1}{2}C_\omega^2\rho_N^2 + \frac{1}{2}C_\rho^2\rho_N^2\delta^2 + \frac{1}{2}\tilde{C}_\sigma^2(m_N^* - M^*)^2 \\ &\quad + \sum_{i=p,n}\frac{2}{(2\pi)^3}\int_0^{k_{F\,i}} d^3k\; E^* + \mathcal{E}_{non}, \qquad (2)\end{aligned}$$

where $C_\omega = g_\omega^*/m_\omega^*$, $C_\rho = g_\rho^*/m_\rho^*$, $\tilde{C}_\sigma = m_\sigma^*/g_\sigma^*$, $E^* = \sqrt{\mathbf{k}^2 + {m_N^*}^2}$ with $m_N^* = M^* - g_\sigma^*\sigma$ the effective mass of nucleon, and $k_F$ is the Fermi momentum. Here, the parameters with asterisks denote the density dependence which is determined in specific models according to Brown-Rho scaling [27, 28]. Besides the Brown-Rho scaling, one can also include in the model the nonlinear meson self-interaction terms [29]. Note that if the nonlinear vector meson self-interaction terms are included in the model, the vector meson masses in $C_\omega$ and $C_\rho$ in the form of the energy density as in Eq.(2) are modified to have additional density dependence. The term $\mathcal{E}_{non}$ is the energy density from the nonlinear meson self-interaction terms. In usual nonlinear RMF models, the parameters are not density-dependent [30–32]. However, if the nonlinear vector meson terms are included, the vector meson masses in $C_\omega$ and $C_\rho$ in Eq.(2) are also becoming density-dependent. With Eq.(2), the symmetry energy in the RMF models can be given as

$$E_{sym} = \frac{1}{2}\frac{\partial^2(\mathcal{E}/\rho_N)}{\partial\delta^2} = \frac{1}{2}C_\rho^2\rho_N + \frac{k_F^2}{6E_F^*}, \qquad (3)$$

with $E_F^* = \sqrt{k_F^2 + {m_N^*}^2}$.

For hyperon degrees of freedom, we consider only the $\Lambda$ hyperon for simplicity. In this case, Eq.(1) still holds for hyperonized matter. The nuclear symmetry energy now reads

$$E_{sym} = \frac{1}{2}C_\rho^2\frac{\rho_N^2}{\rho_B} + \frac{k_F^2}{6E_F^*}\frac{\rho_N}{\rho_B}, \qquad (4)$$

where $k_F$ is the nucleon Fermi momentum, $\rho_N$ is the number density of nucleons, and $\rho_B = \rho_N + \rho_\Lambda$. The symmetry energy is now suppressed due to the factor $\rho_N/\rho_B$. On the other hand, as one source term of meson fields, the $\Lambda$ hyperon has led to a moderate decrease to the nucleon effective mass and $E_F^*$ in the kinetic term. Together with the suppressed nucleon Fermi momentum in $E_F^*$, the suppression of the kinetic term can be partially compensated. Nevertheless, the symmetry energy eventually turns out to be suppressed in either the baryon-density or nucleon-density profile. While the formula (4) applies to the case of the given ratio $\rho_\Lambda/\rho_B$, in chemically equilibrated and charge neutral matter where the particle fractions are obtained from solving coupled equations, we may calculate the nuclear symmetry energy using the following relation

$$E_{sym} = \frac{1}{4\delta}(\mu_n - \mu_p)\frac{\rho_N}{\rho_B}, \qquad (5)$$

where $\mu_n$ and $\mu_p$ are the neutron and proton chemical potentials, respectively

$$\mu_i = E_F^* + U_i - \Sigma^0, \;\; i = n, p. \qquad (6)$$

Here, $\Sigma^0$ is the rearrangement term induced by the density dependence of model parameters [27], and $U_i$ are the nucleon vector potentials. Note that the symmetry energy given in Eq.(5) is derived from the parabolic approximation (1) and thus is also defined at $\delta = 0$. With Eq.(5), one can obtain the symmetry energy using the difference of nucleon chemical potentials in asymmetric matter. As the isospin asymmetry parameter $\delta$ runs to vanishing, the formula (5) reduces to Eq.(4).

After the hadron-quark phase transition occurs, hadrons and quarks coexist in a mixed phase. The construction of the mixed phase is based on the mechanical and chemical equilibriums, namely, the Gibbs conditions which are given as [21]

$$\begin{aligned}p^H &= p^Q, \;\; \mu_u = \mu_p/3 - \mu_e/3, \\ \mu_d &= \mu_s = \mu_n/3 + \mu_e/3. \qquad (7)\end{aligned}$$

The pressures of nuclear and quark matter read

$$\begin{aligned}p^H &= \frac{1}{2}C_\omega^2\rho_N^2 + \frac{1}{2}C_\rho^2\rho_N^2\delta^2 - \frac{1}{2}\tilde{C}_\sigma^2(m_N^* - M^*)^2 \\ &\quad + \frac{1}{3}\sum_{i=p,n}\frac{2}{(2\pi)^3}\int_0^{k_{F\,i}} d^3k\;\frac{\mathbf{k}^2}{E^*} \\ &\quad - \Sigma^0\rho_N - \mathcal{E}_{non}, \qquad (8)\\ p^Q &= \sum_{i=u,d,s}\frac{2}{(2\pi)^3}\int_0^{k_{F\,i}} d^3k\;\frac{\mathbf{k}^2}{\sqrt{\mathbf{k}^2 + m_i^2}} - B, \qquad (9)\end{aligned}$$

where $B$ is the bag constant of the MIT model [33]. For convenient narration, we do not include in above equations the $\Lambda$ hyperons whose addition can be referred to Ref. [23]. In actual calculations, we include the strange meson-hyperon interactions. In terms of the quark phase fraction $Y$, the total baryon density can be expressed as

$$\rho_B = \frac{Y}{3}\rho_Q + (1 - Y)\rho_H, \qquad (10)$$

where $\rho_H = \rho_N + \rho_\Lambda$ is the baryon density on the hadronic level and $\rho_Q$ is the quark density. Using Gibbs conditions, one can obtain the quark phase fraction $Y$. The total energy density and isospin asymmetry parameters are written as

$$\mathcal{E} = (1-Y)\mathcal{E}_H + Y\mathcal{E}_Q,\ \alpha = (1-Y)\delta_H + Y\delta_Q, \quad (11)$$

with $\delta_H = (\rho_n - \rho_p)/\rho_N$ and $\delta_Q = (\rho_u - \rho_d)/(\rho_u + \rho_d)$. The energy density in the mixed phase thus depends on the $Y$. In the parabolic approximation, the energy density can be expressed as

$$\mathcal{E}/\rho_B = e_0(\rho_B, Y) + E^H_{sym}(\rho_B, Y)\delta_H^2 + E^Q_{sym}(\rho_B, Y)\delta_Q^2. \quad (12)$$

Because the quark phase fraction depends on the isospin asymmetry, we limit the derivation of the symmetry energy $E^H_{sym}$ in symmetric matter, namely $\alpha = 0$. In this way, the nuclear symmetry energy is defined as $E^H_{sym} = \frac{1}{2}\partial^2(\mathcal{E}/\rho_B)/\partial\delta_H^2$ at $\delta_H = 0$, and the definition of the quark symmetry energy is similarly given as $E^Q_{sym} = \frac{1}{2}\partial^2(\mathcal{E}/\rho_B)/\partial\delta_Q^2$ at $\delta_Q = 0$. Bridged by Gibbs conditions, the quark phase fraction is model dependent and relies on the MIT bag constant. As a result, similar dependencies on the model and bag constant can be delivered to the symmetry energy. As seen from Eqs.(11) and (12), the nuclear symmetry energy may disappear as the quark fraction grows to be unity at high densities.

## III. NUMERICAL RESULTS AND DISCUSSIONS

We use the RMF models SLC and SLCd [28] to investigate the role of hyperons in affecting the nuclear symmetry energy. These two models have the same equation of state of symmetric matter, while the SLCd has a much softer symmetry energy than the SLC. We distinguish two kinds of hyperon interactions: the usual and the separable ones [24]. In the usual case, the ratios ( $X_{\sigma Y}$, $X_{\omega Y}$, and $X_{\rho Y}$) of meson-hyperon couplings to the meson-nucleon couplings are constants, while in the separable case the in-medium nucleon and hyperon potentials are treated separately, leading to the density-dependent ratio parameters. Thus, the hyperon potential in the usual case has a similar medium dependence to the nucleon potential, whereas in the separable case they are different (for details, see Ref. [24]). In this work, we just consider the $\Lambda$ hyperon which is an isoscalar. In principle, we can include the isovector components $(\Sigma^\pm, \Sigma^0)$ and $(\Xi^0, \Xi^-)$ and generally introduce in the energy density the new symmetry energy terms for these isovector components as in Eq.(12). It would be interesting to analyze the properties of the hyperon symmetry energies and the effects on the nuclear symmetry energy. However, in this work we just focus on the effect of the isoscalar $\Lambda$ hyperon by ignoring the complication of the isovector hyperon components, because the $\Lambda$ fraction is usually dominant in nuclear matter.

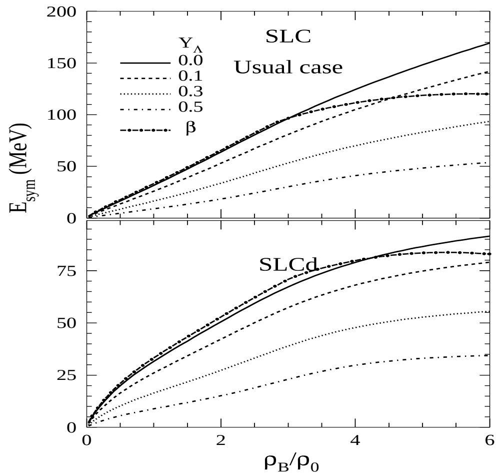


FIG. 1: The symmetry energy as a function of density for various $\Lambda$ fractions in the usual case (For details, see text). The upper panel is for the results with the SLC, while the lower panel displays the results with the SLCd. The label $\beta$ denotes the chemically equilibrated and charge neutral matter. Here, $\rho_0 = 0.16 fm^{-3}$.

In Fig. 1, it shows in the usual case the density profile of the symmetry energy for various $\Lambda$ fractions. The symmetry energy for various $\Lambda$ fractions is calculated in symmetric matter at $\delta = 0$. It is shown in Fig. 1 that the symmetry energy is softened clearly with the increase of the $\Lambda$ fraction. For chemically equilibrated and charge neutral matter, we see that the symmetry energy starts to soften once the $\Lambda$ hyperons appear. In this case, the symmetry energy at lower densities with the SLC is identical with that obtained with $Y_\Lambda = 0$ in symmetric matter, while a small difference appears in results with the SLCd. Shown in Fig. 2 is the symmetry energy for various $\Lambda$ hyperon fractions with the separable case. Except for the chemically equilibrated and charge neutral case, results shown in Fig. 1 and 2 are almost identical. This can be elaborated by Eq.(4) because the nuclear symmetry energy in hyperonized matter is dominantly affected by the hyperon fraction. In the separable case, the hyperon fraction saturates at the certain high density, and the hyperons disappear at very high density. Thus, in the density profile of the symmetry energy, a concave shape forms. We see that the symme-

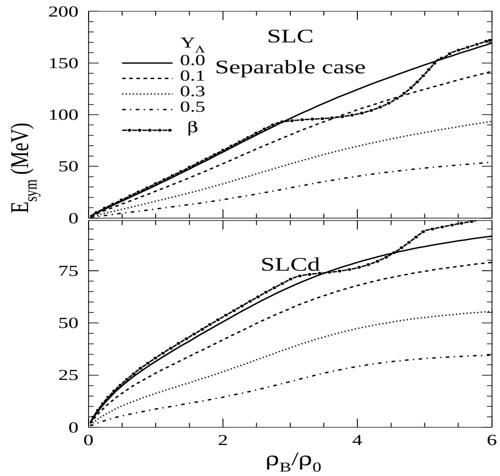


FIG. 2: The same as shown in Fig. 1 but with different density dependencies for the hyperon and nucleon potentials, denoted as the separable case.

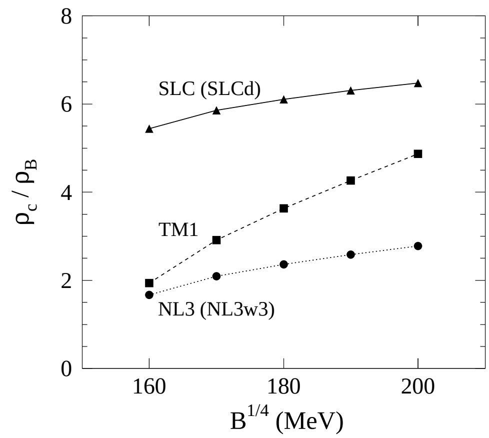


FIG. 3: The critical density of the hadron-quark phase transition vs. the bag constant in symmetric matter for various RMF models. The model and its companion in parentheses predict the same critical density in symmetric matter.

try energy obtained in neutron star matter with the SLCd can deviate from the one calculated at symmetric matter in the high-density region. With a smaller isospin asymmetry predicted in SLC, the similar deviation in the symmetry energy is accordingly smaller. It implies that the parabolic approximation (see Eq.(1)) may produce for highly asymmetric matter some errors at high densities. Also, the error can be partially related to the lepton fractions in neutron star matter.

With the increase of density, the hadron-quark phase transition may occur. In this work, quark matter, regarded as the free fermion gas without interactions, is described with the MIT bag model [33]. In quark matter, we include the up, down and strange quarks. For the hadron phase, besides the density-dependent RMF models SLC and SLCd, we also choose a few nonlinear RMF models in the calculation: NL3 [30], TM1 [31] and NL3w3 [32]. The TM1 parameter set has a much softer vector potential than the NL3 and NL3w3, while the SLC and SLCd have additional rearrangement term, see Eq.(6). Because of these distinctions, these models produce rather different nucleon chemical potentials and quite different critical densities according to Gibbs conditions. Moreover, these models have differences in the symmetry energy. The RMF model NL3w3 has a softer symmetry energy than the NL3. The SLCd and SLC also have different density profile of the symmetry energy, as pointed out above. These specific model factors can affect the occurrence of the phase transition. The mixed phase consists of high-density quark matter and low-density nuclear matter with the quark phase fraction $Y$ being determined according to Gibbs conditions. We do not reiterate here the detailed solutions which can be found in the literature [21]. In the first step, we deal with the phase transition without hyperons. Next, we then include the hyperons.

In Fig. 3, we draw the critical density in symmetric matter with respect to the bag constant for various RMF models. With increasing the isospin asymmetry, the critical density can be lowered rather dramatically. While the details of this issue with the MIT bag model can be found in the literature [25, 34, 35], we focus herein on the phase transition in symmetric matter where we indeed obtain the symmetry energy. It is however noteworthy to point out that the softening of the symmetry energy can play a moderate role in increasing the critical density in asymmetric matter, with the magnitude depending on the bag constant. We see in Fig. 3 that the critical density with the SLC and SLCd is much higher than other models. This is originated mainly from the density-dependent properties induced by the Brown-Rho scaling. Compared to other models in the present work, the SLC and SLCd feature the rearrangement term and are characteristic of a much smaller nucleon effective mass [27]. The resulting nucleon chemical potentials with the SLC and SLCd are clearly smaller than those with other models. With the chemical equilibrium according to Gibbs conditions, the difference in the critical densities, as shown in Fig. 3, can thus be well understood. In addition, the nonlinear RMF model TM1 has a larger critical density than the NL3 and NL3w3. This is also attributed to the smaller nucleon chemical potential due to the softening of the

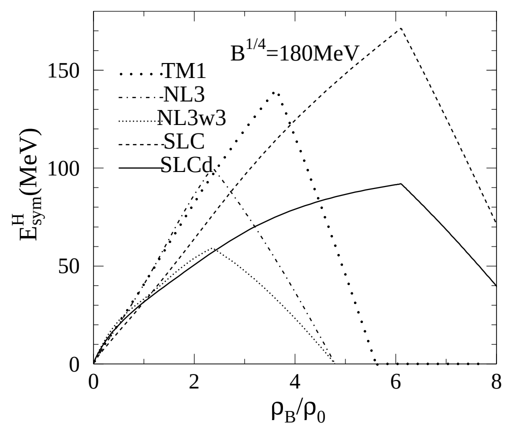


FIG. 4: The nuclear symmetry energy as a function of density in symmetric matter including the hadron-quark phase transition at high densities. The reflection point from rising to dropping corresponds to the critical density for each model.

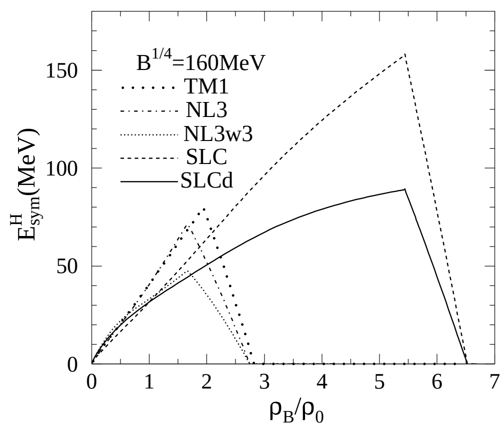


FIG. 5: The same as shown in Fig. 4 but with $B = (160MeV)^4$.

vector potential in TM1 [31]. As seen in Fig. 3, the critical density depends rather sensitively on the bag constant. The rise of the bag constant reduces the pressure of quark matter and thus results in larger critical densities. Note that the critical density with the TM1 and NL3 at $\alpha = 0$ is consistent with that in Ref. [35] as long as we exclude the strange quarks.

Because the critical density and quark phase fraction $Y$ depend on the isospin asymmetry, the symmetry energy in the mixed phase obtained in symmetric matter can not simply be used to predict the properties of asymmetric matter because the quark phase fraction changes with the isospin asymmetry in asymmetric matter. Nevertheless, the symmetry energy obtained in symmetric matter is instructive to exhibit its variation trend in the mixed phase. Shown in Fig. 4 is the nuclear symmetry energy as a function of baryon density with the bag constant $B = (180MeV)^4$. Apparent decrease of the symmetry energy can be observed after the hadron-quark phase transition occurs. With the increase of density, the nucleon phase fraction decreases, which causes a straightforward reduction of the nuclear symmetry energy. As the nucleon phase fraction reduces to zero, the nuclear symmetry energy vanishes.

For a smaller bag constant, the decrease of the symmetry energy starts at lower critical densities for various models. Shown in Fig. 5 is the symmetry energy with $B = (160MeV)^4$. We see that the critical density is around 1.6-2$\rho_0$ for the nonlinear RMF models and the symmetry energy vanishes at densities below $3\rho_0$, while these densities with the SLC and SLCd are also considerably smaller than those at $B = (180MeV)^4$. With the increase of the bag constant, the model difference in the critical density and the vanishing density of the symmetry energy can grow significantly. This can be observed by comparing Figs. 4 and 5, while it is more appreciable for a much larger bag constant, for instance, $B = (200MeV)^4$. Nevertheless, once the hadron-quark phase transition occurs, the decrease of the symmetry energy is definite.

For the quark phase, the quark symmetry energy $E^Q_{sym}$ which reflects the cost in deviating from the flavor symmetric matter starts to have value above the critical density and increases with the rise of the quark phase fraction, as shown in Fig. 6. Here, the quark symmetry energy is defined for the up and down quarks, see Eq.(12). After the quark phase fraction develops soon to be unity that is a value for pure quark matter, the quark symmetry energy grows quite slowly with the density, since without interactions only the kinetic energy contributes to the symmetry energy.

With the inclusion of hyperons, the reconstruction of the chemical equilibrium with quarks results in a different critical density. In Fig. 7, it shows the nuclear symmetry energy in the hadronic and mixed phases for various fractions of $\Lambda$ hyperons with RMF models SLC and SLCd. Here, the bag constant is $B = (160MeV)^4$. The inclusion of $\Lambda$ hyperons suppresses the symmetry energy in the hadronic phase, consistent with those shown in Figs. 1 and 2. For other bag constants and RMF models, the conclusion is qualitatively similar. Namely, the inclusion of $\Lambda$ hyperons suppresses the symmetry energy in hadronic phase, and the decrease of the symmetry energy starts at a little different

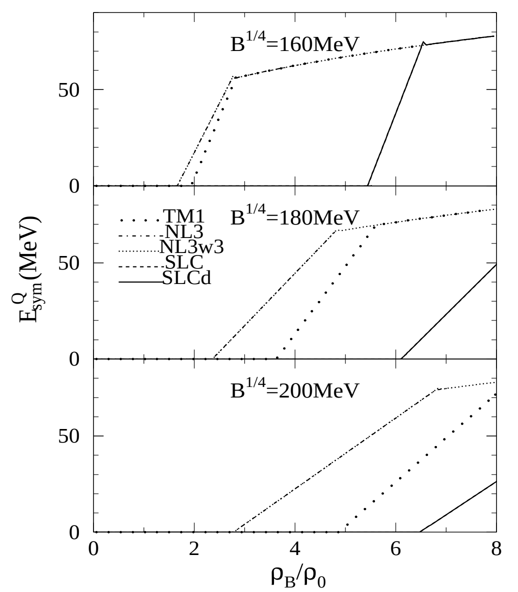


FIG. 6: The quark symmetry energy as a function of density for various bag constants and RMF models. The difference in the symmetry energy exists in the mixed phase for various RMF models, and it disappears in pure quark matter at sufficiently high densities.

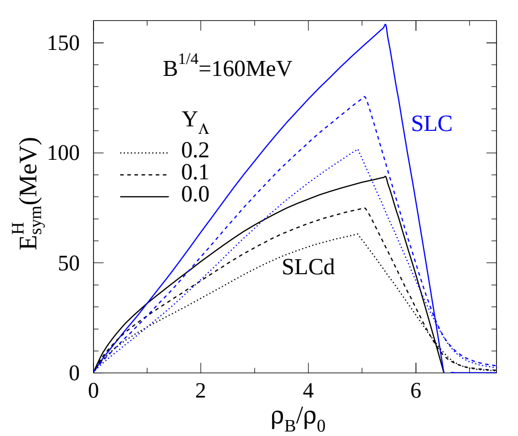


FIG. 7: (Color online) The symmetry energy as a function of density for different Λ-hyperon fractions in hyeronized matter with the hadron-quark phase transition. The RMF models SLC and SLCd are adopted here and the bag constant is $(160MeV)^4$.

critical density. To save space, these numerical results are thus not displayed.

We note that the softening of the symmetry energy in the mixed phase is mostly apparent because once the quark phase fraction can be identified at given densities the nuclear symmetry energy would be extracted appropriately by singling out the effect of suppression factor $(1-Y)$. However, the determination of the $Y$ is strongly model-dependent and far from experimental feasibility. On the other hand, the decreasing factor $(1-Y)$ in the mixed phase largely suppresses the growth of the nucleonic density with the rise of the total density. If the hyperons are taken into account, the situation becomes more complicated. Thus, the extraction of the high-density symmetry energy for pure nucleonic matter is not well grounded once the hadron-quark phase transition occurs. Most likely, the high-density symmetry energy extracted from the heavy-ion collisions would be as soft as that presented in this work as long as a detailed discrimination or calibration is not ready for dynamically evolutional matter. In deed, the extraction of the symmetry energy encounters the finite size effects which can cause the increase of the critical density [25]. However, the decreasing tendency of the nuclear symmetry energy above the critical density will not be altered by the finite size effects.

At last, it would be interesting to point out that our results may provide indications to overcome the difficulty in reproducing the neutron star properties with the EOS featuring a super-soft symmetry energy, while much attention has recently been paid to this difficulty since the super-soft symmetry energy was extracted [13, 36]. However, it is worth mentioning that the appearance of new degrees of freedom that is energetically favored usually softens the equation of state, resulting in a significant decrease of the maximum mass of neutron stars. Recently, the pulsar J1614-2230 was identified rather accurately through the Shapiro delay to have a mass $2M_\odot$ [37], which sets up a lower limit of the maximum mass of neutron stars. This states that the nuclear equation of state should not be softened significantly even with the appearance of new degrees of freedom. A way out is to consider new forms of interactions for new degrees of freedom [24, 38–42]. For quark matter, the imposition of interactions can stiffen the equation of state and hence increase the maximum mass of neutron stars [40–42]. It would be interesting to investigate whether the interactions of quarks have an effect on the nuclear symmetry energy. This deserves subsequent work and is however beyond the scope of the present work.

## IV. SUMMARY

We have studied the effect of Λ hyperons and quarks on the nuclear symmetry energy at high densities with relativistic models. The softening of the nuclear symmetry energy is observed either in chemically equilibrated matter or matter with an given $\Lambda$ fraction. With the inclusion of quark degrees of freedom, we have constructed the isospin symmetric mixed phase according to Gibbs conditions using the RMF models and MIT bag model. The nuclear symmetry energy obtained in the mixed phase reduces quickly with the rise of quark phase fraction. We have recognized that the specific softening depends on the parametrizations of models. Especially, it has a clear dependence on the bag constant of the MIT bag model. Nevertheless, we conclude that the effect of phase transitions is important on the symmetry energy, and for the experimental extraction of the symmetry energy at high densities it is significant and necessary to take into account the effect of phase transitions.

**Acknowledgement**

Authors thank Prof. X. M. Xu for useful discussions. The work was supported in part by the National Natural Science Foundation of China under Grant Nos. 10975033 and 11275048 and the China Jiangsu Provincial Natural Science Foundation under Grant No.BK2009261.

[1] B. A. Li, Phys. Rev. Lett. **85**, 4221 (2000); ibid. **88**, 192701 (2002).
[2] W. Z. Jiang, Y. L. Zhao, Phys. Lett. B **617**, 33 (2005).
[3] B. A. Li, L. W. Chen, and C. M. Ko, Phys. Rep. **464**, 113 (2008).
[4] J. M. Lattimer and M. Prakash, Phys. Rep. **333**, 121 (2000); Science **304**, 536 (2004); Phys. Rep. **442**, 109 (2007).
[5] C. J. Horowitz, J. Piekarewicz, Phys. Rev. Lett. **86**, 5647 (2001).
[6] A. W. Steiner, J. M. Lattimer and E. F. Brown, Astrophys. J. **722**, 33 (2010).
[7] L. W. Chen, C. M. Ko, B. A. Li and J. Xu, Phys. Rev C **82**, 024321(2010).
[8] W. Newton, M. Gearheart, and B. A. Li, arXiv:1110.4043.
[9] A. W. Steiner and S. Gandolfi, Phys. Rev. Lett. **108**, 081102 (2012).
[10] M. B. Tsang, et al. Phys.Rev. C **86**, 015803 (2012).
[11] D. H. Wen, W. G. Newton, and B. A. Li, Phys. Rev C **85**, 025801 (2012).
[12] J. M. Lattimer, and Y. Lim, ArXiv:1203.4286v1
[13] Z. G. Xiao, B. A. Li, L. W. Chen, G. C. Yong, and M. Zhang, Phys. Rev. Lett.**102**, 062502 (2009).
[14] Z. Q. Feng and G. M. Jin, Phys. Lett. B **683**, 140 (2010).
[15] P. Russotto, W. Trauntmann, Q. F. Li, et al., Phys. Lett. B **697**, 471 (2011).
[16] C. Xu and B. A. Li, Phys.Rev. C **81**, 064612 (2010).
[17] I. Vidana, A. Polls, and C. Providencia, Phys. Rev. C **84**, 062801(R) (2011).
[18] R. Brockmann and R. Machleidt, Phys. Rev. C **42**, 1965 (1990).
[19] H. Q. Song, M. Baldo, G. Giansiracusa, and U. Lombardo, Phys. Rev. Lett. **81**, 1584 (1998).
[20] M. Prakash, I. Bombaci, M. Prakash, P. J. Ellis, J. M. Lattimer, and R. Knorren, Phys. Rep. **280**, 1 (1997).
[21] N. K. Glendenning, Phys. Rep. **342**, 393 (2001).
[22] T. Takatsuka, S. Nishizaki, Y. Yamamoto, and R. Tamagaki, Prog. Theor. Phys. Suppl. **146**, 279 (2002).
[23] W. Z. Jiang, Phys. Lett. B **642**, 28 (2006).
[24] W. Z. Jiang, B. A. Li and L. W. Chen, Astrophys. J. **756**, 56 (2012).
[25] M. Di Toro, A. Drago, T. Gaitanos, V. Greco, and A. Lavagno, Nucl. Phys. A **775**, 102 (2006).
[26] M. Di Toro, B. Liu, V. Greco, V. Baran, M. Colonna, and S. Plumari, Phys. Rev. C **83**, 014911(2011).
[27] W. Z. Jiang, B. A. Li and L. W. Chen, Phys. Lett. **B653**, 184 (2007).
[28] W. Z. Jiang, B. A. Li and L. W. Chen, Phys. Rev. C **76**, 054314 (2007).
[29] C. Song, Phys. Rep. **347**, 289 (2001).
[30] G. A. Lalazissis, J. König, and P. Ring, Phys. Rev. C **55**, 540 (1997).
[31] Y. Sugahara and H. Toki, Nucl. Phys. A **579**, 557 (1994).
[32] W. Z. Jiang, Phys. Rev. C **81**, 044306 (2010).
[33] A. Chodos, R. L. Jaffe, K. Johnson, C. B. Thorn, and V. F. Weisskopf, Phys. Rev. D **9**, 3471 (1974).
[34] G.Y. Shao, M. Di Toro, B. Liu, et. al., Phys. Rev. D **83**, 094033 (2011).
[35] R. Cavagnoli, C. Providencia,and D. P. Menezes, Phys. Rev. C83, 045201 (2011).
[36] D. H. Wen, B. A. Li, and L. W. Chen, Phys. Rev. Lett. 103, 211102 (2009).
[37] P. B. Demorest, T. Pennucci, S. M. Ransom, M. S. E. Roberts, and J. W. T. Hessels, Nature **467**, 1081 (2010).
[38] I. Bednarek, P. Haensel, J. L. Zdunik, M. Bejger, and R. Manka, arXiv:1111.6942 [astro-ph.SR].
[39] S. Weissenborn, D. Chatterjee, J. Schaffner-Bielich, Phys. Rev. C **85**, 065802 (2012).
[40] M. Alford, M. Braby, M. Paris, and S. Reddy, Astrophys. J.**629**, 969 (2005).
[41] S. Weissenborn, I. Sagert, G. Pagliara, M. Hempel, and J. Schaffner-Bielich, Astrophys. J. **740**, L14 (2011).
[42] L. Bonanno and A. Sedrakian, Astron. Astrophys. **539**, A16 (2012).